

Dalton Transactions

Accepted Manuscript

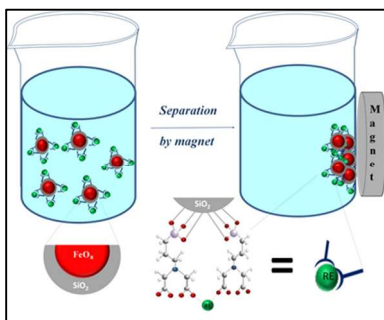


This is an *Accepted Manuscript*, which has been through the Royal Society of Chemistry peer review process and has been accepted for publication.

Accepted Manuscripts are published online shortly after acceptance, before technical editing, formatting and proof reading. Using this free service, authors can make their results available to the community, in citable form, before we publish the edited article. We will replace this *Accepted Manuscript* with the edited and formatted *Advance Article* as soon as it is available.

You can find more information about *Accepted Manuscripts* in the [Information for Authors](#).

Please note that technical editing may introduce minor changes to the text and/or graphics, which may alter content. The journal's standard [Terms & Conditions](#) and the [Ethical guidelines](#) still apply. In no event shall the Royal Society of Chemistry be held responsible for any errors or omissions in this *Accepted Manuscript* or any consequences arising from the use of any information it contains.

Graphical abstract image**Graphical abstract Synopsis**

The IDA-RE³⁺ complexation of RE³⁺ on the surface of hybrid silica adsorbent occurs at neutral or weakly acidic conditions apparently not via chelation but via concerted action of the negatively charged carboxylate oxygen atoms opening for enhanced selectivity.

ARTICLE

Molecular insights into selective action of a magnetically removable complexone-grafted adsorbent

Cite this: DOI: 10.1039/x0xx00000x

Received 00th January 2012,
Accepted 00th January 2012

DOI: 10.1039/x0xx00000x

www.rsc.org/

Elizabeth Polido Legaria,^a Seda Demirel Topel,^a Vadim G. Kessler^{a*} and Gulaim A. Seisenbaeva^{a*}

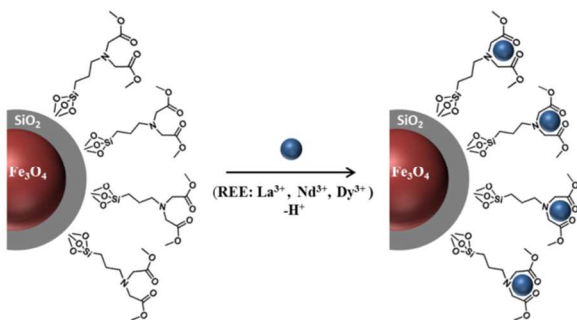
Binding and release of trivalent Rare Earth Element (REE) cations (Dy^{3+} , Nd^{3+} and La^{3+}) from solutions by new fully characterized magnetic nano adsorbent material, consisting of iminodiacetic acid ligand (H_2IDA) grafted onto SiO_2 covered $\gamma\text{-Fe}_2\text{O}_3$ nanoparticles was investigated. The nano adsorbent revealed slightly higher capacity towards heavier REE and appreciable selectivity especially on desorption. It was found that the composition of the surface complex was $\text{RE}^{3+}:\text{L} = 1:1$. The complexation of the molecular H_2IDA with RE^{3+} in this ratio under non-basic conditions was therefore investigated by X-Ray Crystallography to produce relevant molecular models. Unexpectedly big difference in coordination numbers and binding mode of IDA along with distinct analogies in packing of the ligand molecules in the obtained 2D-coordination polymer structures provided valuable insights into possible reasons of the observed selectivity.

Introduction

Rare earth element (REE) based materials are gaining increasing importance due to their wide range of applications such as high field strength magnets,¹ sensing,² electro optical devices,³ catalysis⁴ and unique materials.⁵ This increased demand for the REE resulted in their increased production from ores (i.e. mining) and also in strong research focus on development of technologies for their recycling. Therefore, an effort has been made to improve procedures for separation and purification of REE from wastewaters and ores.⁶ These techniques include in particular high affinity sorbents for sequestering the lanthanides from dilute industrial waste streams or the removal/sorption and extraction from mining leachates. For instance, hydroxypyridinone (HOPO) and ethylenediaminetetraacetic acid (EDTA) ligands proved as effective chelating reagents for complexation with actinide and lanthanides in aqueous solution.⁷ On the other hand, a sorbent material should be economical for the industrial purposes, having reproducible capacity to be reused in several cycles and minimizing the burden to the environment after its use.⁸ In this point, iron oxide nanoparticles are offering many advantages due to their magnetism – an attractive physical property for application in adsorbents permitting facile magnetic removal. Especially in environmental applications, iron oxide nanoparticles (FeO_x NP) have good stability and less toxicity compared to their metallic analogues like iron and cobalt.⁹ Hu and co-workers¹⁰ have synthesized silica coated Fe_3O_4 NP functionalized with γ -mercaptopropyltrimethoxysilane for extraction of Cd^{2+} , Cu^{2+} , Hg^{2+} and Pb^{2+} ions from environmental and biological samples. Trindade and co-workers¹¹ have studied magnetic removal of Hg^{2+} ion from

water using dithiocarbamate grafted $\text{Fe}_3\text{O}_4\text{-SiO}_2$ nanoparticles. The uptake capacity for Hg^{2+} achieved 74% even at contaminant level as low as 50 $\mu\text{g/l}$. Jang and co-workers¹² reported the synthesis of Fe_3O_4 nanoparticles encapsulated with poly(3,4-ethylenedioxythiophene) and studied their efficiency to remove Ag^+ , Hg^{2+} and Pb^{2+} ions from aqueous solutions. According to the literature, the adsorption of heavy metals combined with ligand conjugated magnetic separation has recently become extensively used in water treatment and environmental cleanup.¹³ Very little, however, has been reported on removing trivalent rare earth ions (RE^{3+}) from industrial waste water or mining leachates by using iron oxide nanoparticles. The strategic importance of developing a general approach capable to result in a new technology for separation of REE based on application of selectively acting hybrid magnetic nanoparticles has been recognized by the European Union resulting in including this task in the work plan of the EURARE EU FP-7 Project that supported this work. It is generally necessary to coat Fe_3O_4 (and more generally, iron oxide) NP surface with an organic or inorganic shell in order to protect it from chemical degradation or agglomeration in the environments in which they should be used.¹⁴ Among different kinds of coating materials, silica has been studied most intensively possessing several advantages arising from its stability under acidic aqueous conditions. In a recent study it has been demonstrated that coating of iron oxide nanoparticles with Stober silica transforms quantitatively Fe_3O_4 into $\gamma\text{-Fe}_2\text{O}_3$ without major loss of magnetic characteristics and provides magnetic particles stable even in concentrated strong acids when the molar ratio $\text{SiO}_2:\text{FeO}_x \geq 6$ ($\text{SiO}_2:\text{Fe}_3\text{O}_4 \geq 18$). The magnetic susceptibility of the thus produced material remained at level of ca. 6 emu/g matching industrial requirements for

magnetic separation.¹⁵ It offers not only protection of the magnetic cores - it prevents also the direct contact of the magnetic core with additional agents linked to the surface and enhances its biocompatibility, hydrophilicity, dielectric properties etc.¹⁶ Furthermore, it also facilitates surface modification due to the silanol groups (-SiOH) on its surface.¹⁷



Scheme 1. Proposed design concept for magnetic nanosorbent material according to common understanding of complexone-binding.⁷

In this study, we intended not only to demonstrate a cost-efficient approach to a new magnetic nano adsorbent. Our principal aim was to understand the chemistry of REE binding to complexone-bearing nanoparticles and to provide insight into molecular origins of possible selectivity in this process. The widespread idea of binding through chelation as explained in Scheme 1 turned out to be erroneous in this case. The obtained X-ray single crystal structures of the molecular models revealed unexpectedly coordination via concerted action of the grafted anions and highly varied coordination for cations with slightly different sizes in the coordination polymer like surface layers.

Results and discussion

Optimization of NP synthesis and effects of reaction parameters.

Numerous chemical methods can be used to synthesize magnetic nanoparticles such as microemulsion,¹⁸ sol-gel synthesis,¹⁹ sonochemical reactions,²⁰ hydrothermal reactions,²¹ hydrolysis and thermolysis of precursors,²² flow injection²³ and electrospray synthesis.²⁴ The most common method for the preparation of magnetite nanoparticles is the chemical co-precipitation of iron salts.^{25, 26} The co-precipitation technique is probably the simplest and the most efficient chemical pathway to obtain magnetic particles. Iron oxides are generally prepared by hydrolysis of stoichiometric mixture of ferrous and ferric salts in aqueous medium. In this work, we synthesized the Fe₃O₄ nanoparticles according to the co-precipitation method under non-oxidizing environment using a stoichiometric Fe³⁺:Fe²⁺ ratio of 2:1, in aqueous medium on addition of ammonia solution.

In order to coat the surface of iron oxide nanoparticles with silica, one can use either microemulsion or the alkaline hydrolysis of tetraethyl orthosilicate (TEOS) (known as Stoeber method).¹⁷ The Stoeber approach is a facile and effective process to synthesize uniform spherical colloid silica particles in ethanol aqueous solution, and was chosen therefore in the present work. For this purpose, firstly uniform Fe₃O₄ NPs were introduced into a classical Stoeber solution containing TEOS, ethanol and ammonia catalyst, and thus uniform amorphous silica shell can homogeneously be grown on the magnetite/maghemite to obtain core shell FeO_x-SiO₂ micro/nanospheres depending on the reaction conditions.

In the first procedure (*I*), we performed the synthesis in 40 mL of ethanol with a mmol ratio of NH₄OH/TEOS 23:1 and TEOS/Fe₃O₄ 30:1 at room temperature for 2 hours yielding ca 800 nm particle sizes according to SEM measurements (Fig.1, Table 1).

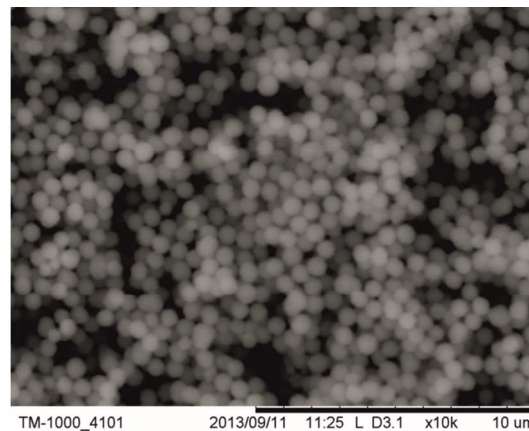


Fig. 1. SEM image of γ -Fe₂O₃-SiO₂ nanoparticles synthesized under the conditions-*I*.

However, for our purposes it was important to synthesize smaller particles possessing larger surface area which allows binding more organic ligands and thus increasing the possibility of coordination with rare earths in solution. Therefore, we carried out the second procedure (*II*) with lower ammonia:TEOS ratio (NH₄OH/TEOS=8:1) and lower TEOS:Fe₃O₄ concentration (TEOS/Fe₃O₄=18:1) in higher volume of ethanol (160 mL) and also in the presence of milli-Q water (32 mL) (Table 1).

Table 1 Reaction parameters for the synthesis of Fe₃O₄-SiO₂ nanoparticles.

No	Fe ₃ O ₄ (mmol)	H ₂ O (mL)	Ethanol (mL)	NH ₄ OH (mmol)	TEOS (mmol)	Hours (h.)	Particle Size (nm)
<i>I</i>	0.4	-	40	270	11.8	2	800
<i>II</i>	0.4	32	160	53.4	7.0	20	100

Under procedure (*II*) conditions, we obtained particles with an average diameter of 100 nm (\pm 15nm) according to TEM results (Fig.2A).

Stoeber technique reveals rather uniform coating around the nanoparticle clusters with the formation of approximately 25 nm silica thick silica layer (Fig.2B). The fringes, which indicate a crystalline form of iron oxide with cubic spinel structure (FeO_x NPs), can easily be seen at higher resolution (Fig. 2C). EF-TEM image shows the mapping of Fe and Si elements in green and red colors respectively (Fig. 2D), demonstrating that the silica layer in case of procedure (*II*) is emerging around aggregates of iron oxide nanoparticles.

For industrial purposes, it is very important that the synthesized iron oxide nanoparticles covered with silica are resistant under the acidic conditions during repeated the process of separation of lanthanides from aqueous solution. Therefore leaching tests for γ -Fe₂O₃-SiO₂ nanoparticles have been carried out in 0.5 % KSCN in 0.1 M HNO₃.

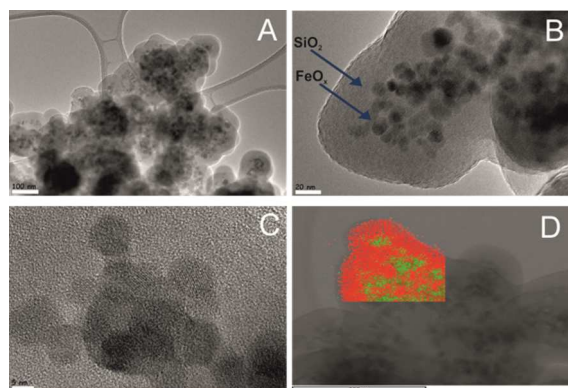


Fig. 2. HR-TEM images of γ -Fe₂O₃-SiO₂ nanoparticles (scale bar is 100, 20 and 5 nm for A, B and C respectively) D is the image of EF-TEM mapping.

It could be noted that within more than 6 months there hasn't been any detectable iron leaching to the solution from the NP sample prepared under the synthesis-II conditions (TEOS/Fe₃O₄=18:1). For comparison, we also showed the leaching from the sample prepared at the ratio TEOS: Fe₃O₄ = 0.125 (Fig. 3B- right image) which gives dark red color when iron (III) complexes with thiocyanate form in the acidic solution (equations 1, 2).



It was also observed that after covering the Fe₃O₄ NPs with silica, the black color of the material turned to brownish and became dark beige after IDA grafting onto the surface of silica.

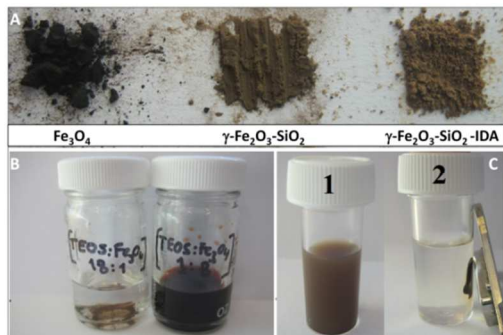


Fig. 3. **A:** Synthesized nanoparticle having different colors indicating transformation from Fe₃O₄ into γ -Fe₂O₃, **B:** Leaching test images of silica covered γ -Fe₂O₃ NPs, **C:** (1) Dispersed γ -Fe₂O₃-SiO₂ NPs in ethanol, (2) Removal of γ -Fe₂O₃-SiO₂ NPs with magnet.

This color change is indicative of the transformation of Fe₃O₄ into γ -Fe₂O₃ (Fig. 3A) as it could be expected from the earlier XANES studies of iron oxide transformation under Stoerber synthesis.¹⁵

XRD of the produced core-shell material was consistent with conservation of a cubic spinel structure typical for both Fe₃O₄ and γ -Fe₂O₃ (see Fig. FS1) A magnet placed in contact with the dispersed γ -Fe₂O₃-SiO₂ NP in solution in ethanol resulted in that all the dispersed particles could be collected within less than a minute leaving a clear solution (see Fig. 3C).

Surface bonding and composition.

In order to confirm the covalent bonding of IDA to the surface of γ -Fe₂O₃-SiO₂ nanoparticle, FTIR spectroscopy was applied.

According to Fig. 4(A), there is a strong absorption band at 578 cm⁻¹ belongs to a characteristic band of the Fe-O stretching vibrations in FeO_x NPs. Two bands at 3400 and 1635 are attributed to the stretching and bending vibrations of O-H bond from residual water in the sample. After covering by silica, the characteristic bands appeared at 1096, 956, 800 and 464 cm⁻¹ attributed to asymmetric stretching vibration of Si-O-Si, stretching vibration of Si-OH, symmetric stretching vibration of Si-O-Si and bending vibration of Si-O-Si, respectively (Fig. 4(A1)).

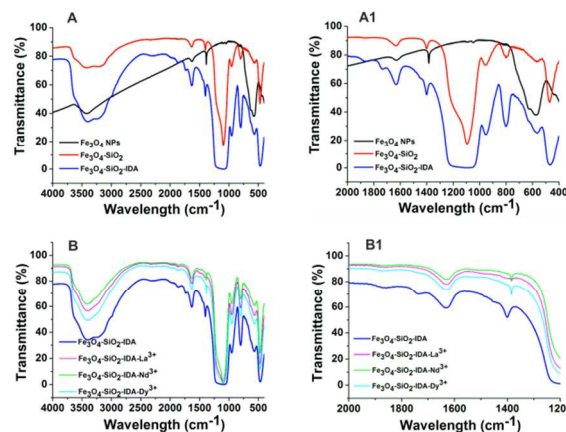


Fig. 4. FTIR spectra of the Fe₃O₄, γ -Fe₂O₃-SiO₂, γ -Fe₂O₃-SiO₂-IDA (A and A1) and γ -Fe₂O₃-SiO₂-IDA-RE³⁺ in comparison with γ -Fe₂O₃-SiO₂-IDA (B and B1).

The Fe-O stretching vibration was shifted to lower frequency (562 cm⁻¹). After iminodiacetic acid (IDA) been grafted onto silica layer of FeO_x NPs, new bands appeared at 1733 cm⁻¹ belonging to the C=O fragment in the carboxylic group which proves that IDA is bonded covalently to the surface.

TGA (thermo gravimetric analysis, see Fig FS2) measurement for γ -Fe₂O₃-SiO₂-IDA was performed to estimate the amount of the surface bound ligand. The mass loss occurs in 3 major steps: first process connected apparently with evaporation of surface adsorbed solvents (water, ethanol and toluene) occurs in the temperature range 25-150°C and is associated with the loss of 5.2 % of the total weight. The second better defined step occurs in the interval 220°C to approximately 400°C after a plateau where the material is thermally stable and corresponds to release of 4.4 %. It is associated with the thermal destruction of the ligand.

The weight loss continues slowly even at higher temperature with the loss of 1.2% more, which reflects most probably the cracking of the residual surface alkyl siloxane species.²⁷ The thermal decomposition of the pure iminodiacetic acid investigated by TGA-MS method²⁸ (see also Fig. FS3 for the TGA-FTIR data obtained in this work) occurs in a highly reproducible manner in 3 steps, where the first at 217-252°C is associated with release of water through formation of an anhydride, the second at 280-338°C is associated with the decarboxylation of the anhydride with release of CO₂ and third less defined step at 400-600°C corresponds to the cracking of the residual material.

The weight loss of 5.6 % in the higher temperature steps, corresponding to the decomposition of the grafted organic ligand, permits to estimate its amount to be about 0.29 mmol/g of adsorbent.

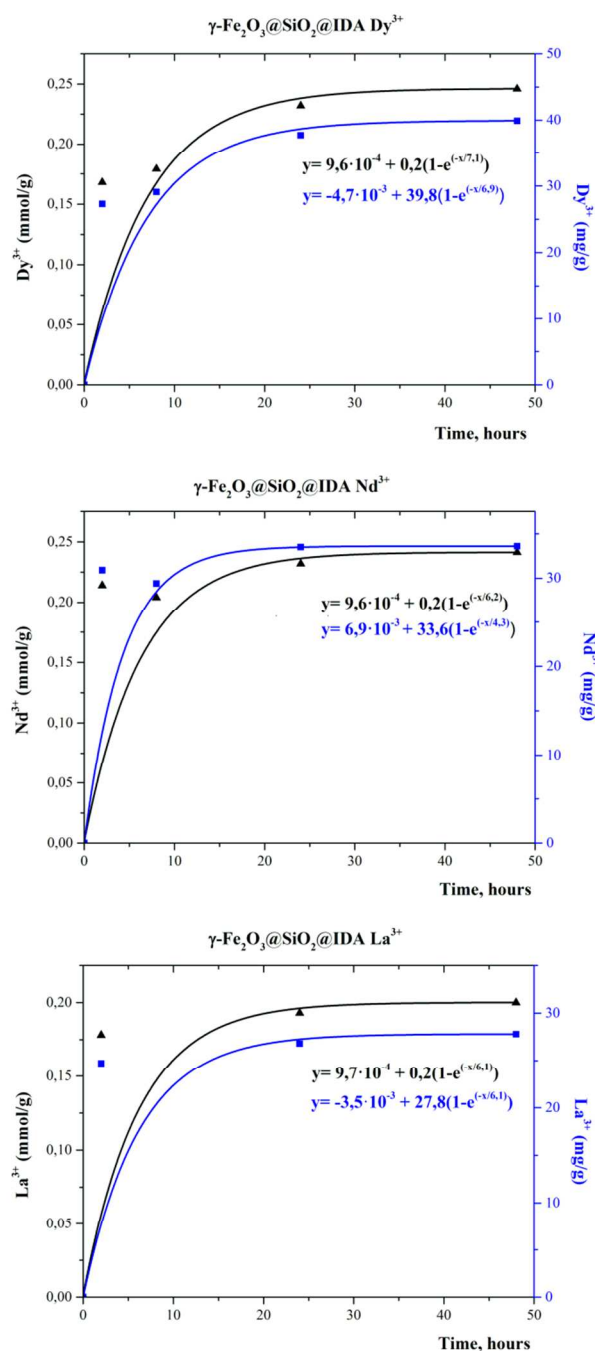


Fig. 5. Kinetic curves of Dy^{3+} , Nd^{3+} and La^{3+} static sorption process on $\gamma\text{-Fe}_2\text{O}_3\text{-SiO}_2$ NPs (in mmol/g in black and mg/g in blue).

It is interesting to note that the decomposition of the molecular model complexes 1 and 2 (Figs. FS4 and FS5) follows the same pattern in temperature regime as the surface grafted ligand: an abrupt step starting at below 50°C and finishing at $200\text{-}250^\circ\text{C}$ is associated with release of “free” water in the structures, while the subsequent decomposition of the ligand proceeds in 3 steps less well defined compared to the pure ligand, but associated with the same types of transformations and is completed just above 600°C .

Static adsorption of Dy^{3+} , Nd^{3+} and La^{3+} ions determined by complexometric titration.

Complexometric titration with Trilon B was carried out in order to test the (Dy^{3+} , Nd^{3+} and La^{3+}) adsorption capacity of the $\text{Fe}_3\text{O}_4\text{-SiO}_2$ NPs towards REE. Kinetic curves show a quick achievement of the adsorption equilibria (Fig. 5) reaching in all the three investigated cases more than 65% of the maximum uptake in 2 hours.

Uptake capacity is, for the three lanthanide ions very reasonable and effective for static sorption processes, resulting in an efficient material for adsorption (Fig. 5). The best uptake capacity was achieved for Dy^{3+} , with a maximum uptake of 0.25 mmol/g (equivalent to 40 mg Dy^{3+} /g), whereas maximum uptake was 0.23 mmol/g for Nd^{3+} (equivalent to 33.6 mg Nd^{3+} /g) and 0.20 mmol/g for La^{3+} (equivalent to 27.8 mg La^{3+} /g). These values sound very reasonable in relation to the estimated amount of grafted ligand (0.26 mmol/g) permitting to estimate the composition of the forming surface complex to be of $\text{RE}^{3+}:\text{L} = 1:1$.

The amounts of RE ions adsorbed under static conditions were comparable but distinctly different with increased capacity towards heavier ones possessing smaller ionic radius. This indicated possibility of selectivity in adsorption from complex solutions. In order to investigate the selectivity of the produced adsorbent it was applied for extraction from solutions containing pairs of RE ions in 1:1 ration.

The particles saturated by RE cations were then subjected to desorption at $\text{pH} = 3.0$ and at $\text{pH} = 1.0$. The results of analysis for metal ratios are summarized in Table 2.

Table 2 Capacity and selectivity in adsorption and desorption of RE cations.

	Dy : Nd ratio	Dy : La ratio
Particles obtained after adsorption at neutral pH	3.9 : 1	4.2 : 1
Particles obtained after desorption at $\text{pH} = 3$	5.9 : 1	81 : 1
Particles obtained after desorption at $\text{pH} = 1$	1.3 : 1	1.8 : 1
Total uptake capacity (by titration), mmol/g	0.242	0.275

The developed adsorbents thus display quite appreciable selectivity. The enrichment factor in adsorption for both the Dy-Nd and Dy-La pairs in case of IDA-bearing particles in our case is quite close to that observed for the La-Dy pair in the use of silica grafted by Ethylene Diamine Triacetic acid in the work of Binnemans et al.^{7b} The desorption at $\text{pH} = 3.0$ does not influence significantly the Dy:Nd ratio but enhances greatly the Dy:La ratio, which opens prospects for efficient separation of RE cations exploiting pH-dependent desorption.

Crystal and molecular structures of the molecular model compounds.

In the view that RE^{3+} ionic radii vary not very drastically it appeared rather interesting to get insight into possible reasons for the observed pronounced and pH-dependent selectivity. The structures of trivalent RE ion complexes with imino diacetic acid (H_2IDA) have become an object of close attention recently in connection with the prospect of obtaining luminescent coordination polymers. The structures generated for this purpose were produced hydrothermally using $\text{RE}^{3+}:\text{IDA}$ ratios 3:1,^{29a} or approximately 3:2.^{29b} In these compounds that are isostructural for the whole lanthanide series the metal centers

are coordinated by 4 chelating and two bridging carboxylate groups (coordination number 9) and are not bearing hydrating water molecules. The coordination polymer forms 3D-structure with huge hexagonal pores making possible an efficient relaxation of the structural tension that can be caused by different size of the metal cations. Relevance of these structures for discussion of the surface complexes on nanoadsorbents is highly questionable.

Much more relevant might appear the works of Oskarsson et al.³⁰ who investigated the complexation at room temperature the interaction of rare earth chlorides with 1.5 eq of H₂IDA. The reaction products turned even in this case three-dimensional coordination polymers and were also isostructural for the whole lanthanide series. The coordination sphere of the RE³⁺ cation in the obtained products with composition formulated as Nd₂(IDA)₃·2HCl·7H₂O comprised one carboxylate group bound in chelating mode, four oxygen atoms of carboxylate bridging functions and one water molecule resulting in quite low total coordination number 7 for all RE³⁺. It was supposedly that the low coordination number in the latter structure permitted it to accommodate metal cations of slightly different size.

In our study we decided to focus on potential RE³⁺:IDA = 1:1 complexes in the view that it was this composition that corresponded to the maximum adsorption capacity of the surface layers. We have also applied nitrate salts as reagents in the view that most promising eudialite REE ores in Sweden can easily be solubilized by nitric acid leaching. The selected approach turned successful and resulted in isolation of compounds [Dy(HIDA)(NO₃)(H₂O)]⁺(NO₃)⁻·(H₂O) (**1**) and [La₂(HIDA)₂(H₂O)₈]⁴⁺(NO₃)₃(HIDA)⁻ (**2**). The composition of the cationic polymer network is in fact analogous and features a layer-type structure with RE³⁺:IDA = 1:1 ratio, being thus potentially quite relevant for the discussion of bonding on the surface of nanoparticles. The IDA units there are grafted covalently through an alkyl group attached to the nitrogen atom of the ligand. As the size of the stabilized particles is 70–80 nm, i.e. 700–800 Å, their surface can reliably be approximated as practically planar for the emerging ligand layers.

The crystal structures of compounds **1** and **2** appear on the first glance, however, very different (see Fig.6). The Dy³⁺-derived **1** has centrosymmetric triclinic structure in which the octa-coordinated Dy atoms occupy a general position. The La³⁺-derived **2** has much more symmetric orthorhombic structure also possessing a center of symmetry, where the La atoms are located. Even molecular structures display a number of differences. In **1** the coordination number of Dy atoms is 8, including 4 oxygen atoms of bridging IDA molecules, 2 oxygens from a chelating nitrate ligand, and 2 oxygen atoms from coordinated water molecules. The coordination sphere of the La atoms in **2** is constructed in a more complex way. The La atoms are deca-coordinated with 2 chelating carboxylate groups occupying 4 of the 10 places. Two more are taken by oxygen atoms of bridging carboxylate groups, and the last 4 – by oxygen atoms of coordinated water molecules.

The nitrate anions in case of **2** are not forming complexes with metal cations at all, but are non-coordinated counter-ions. It is interesting to note that while in **1** the IDA molecules are only located in the coordination sphere of the REE atoms as mono-anions, in **2** they even have partially replaced the nitrate anions (statistically, one half IDA⁻ (–OCOCH₂NH₂(+)CH₂CO⁻) and one-and-a-half nitrate anion per each metal atom).

In both **1** and **2** the imino groups of IDA-anions are protonated, which is relevant for modeling the formation of surface complexes of REE to be adsorbed from neutral or weakly acidic

media. What is especially fascinating and directly relevant for discussion of the reactivity of hybrid sorbents is that the thus formed complexes reveal a common general feature: the REE cations and IDA anions form not separate chelated centers, but planar 2D coordination polymers, where the IDA anion is symmetric, linear and bridging between the REE atoms.

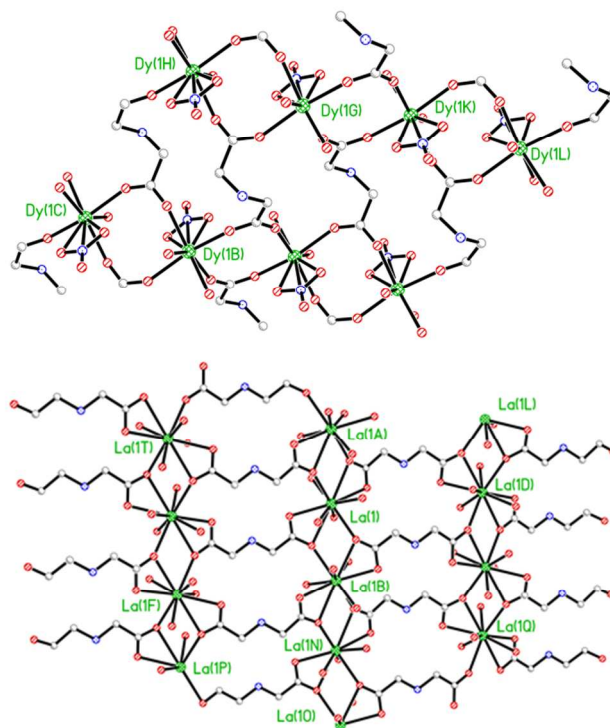


Fig. 6. The structures of 2D coordination polymers as models for binding the REE in the surface layers with covalently grafted IDA molecules: compound **1** above and compound **2** – below.

The ligand is bearing one proton fixed at the nitrogen atom and the metal center has a 2+ residual charge. The binding efficiency is resulting thus from a concerted action of several anions in a layer. It is logical to imagine that analogous construction should emerge on the adsorption of REE onto the surface of nanoparticles bearing grafted IDA ligands under neutral or weakly acidic pH conditions. In this sense it is interesting to try to track the affinity of hybrid adsorbents with covalently grafted functions to the structural features of the investigated molecular models. In the structure of **2** the increased ionic radius of La requires for its formation a considerably denser packing of the IDA⁻ anions. The distance between nitrogen atoms of the organic functions is in this case 4.983(8) Å. The analogous distance in the structure of **1**, where the coordination number of metal atoms is considerably lower, and the packing of ligands is less dense, is 6.365(8) Å. The density of packing of the IDA-ligands on the surface of real hybrid structure is apparently relatively low. Even if the grafted ligands turn to belong to neighboring Si atoms generated by condensation of (EtO)₃Si(CH₂)₃NH₂ precursors (which is of low probability), the distance between the nitrogen atoms will in the best case approach about to about 6–6.5 Å as it can be deduced from the available metallasilsesquioxane models generally considered as representative for the molecular structures on the surface of amorphous silica and silica nanoparticles (see Fig. 7).³¹

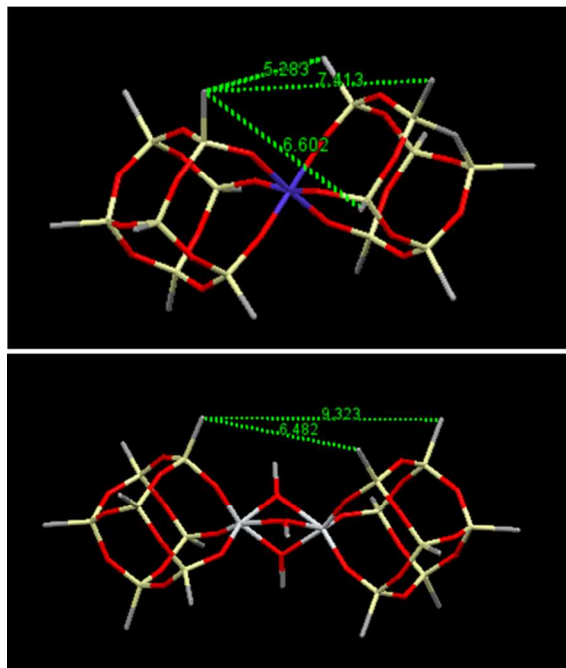


Fig. 7. Distances between adjacent RSiO_3 alkylsiloxane functions in the structures of metallasilsesquioxanes, $\text{Co}[\text{R}_7\text{Si}_7\text{O}_{12}]_2$ (above)^{31a} and $[\text{R}_7\text{Si}_7\text{O}_{12}]\text{Ti}(\text{OR})_2(\text{ROH})\text{Ti}[\text{R}_7\text{Si}_7\text{O}_{12}]$ (below).^{31c}

Formation of a uniform ligand layer will be a result from monolayer coverage of the surface of the particles likely to follow a regular attachment pattern. Lower density of ligands will favour the stronger binding of cations not requiring higher coordination numbers, which then will make such adsorbents relatively more selective towards heavier REE.

This, in fact, is exactly what is observed in both the sorption capacity and in the selectivity studies! The potential loading of the adsorbent increases quite noticeably with the decrease in the size of the cation, reaching only 0.20 mmol/g for La^{3+} , but 0.23 mmol/g for Nd^{3+} and already 0.25 mmol/g (practically saturation with respect to the amount of grafted ligand 0.26 mmol/g according to TGA) for Dy^{3+} , indicating formation of surface complexes with 1:1 composition. The selectivity is also distinctly in favor of cations with smaller ionic radii compared to those with higher ones. It is worth noting that the proposed adsorbent based on IDA as ligand has from the molecular structure of complexes point of view a potentially strong advantage in selectivity over more elaborate complexone-derived ones. It has been clearly demonstrated that nitrilotriacetate (NTA), ethylenediaminetetraacetate (EDTA) and diethylenetriaminepentaacetate (DTPA) all form practically isostructural chelates at weakly acidic pH,³² making separation based on solely the complexation constants less efficient. The IDA ligand binds RE cations via concerted action, opening for much larger differences in selectivity as demonstrated here.

Conclusions

The investigation of IDA- RE^{3+} complexation by single crystal X-Ray technique provided valuable insight into the possible mechanism of IDA and lanthanide (Dy, Nd and La) binding on the surface of hybrid silica adsorbent. The binding at neutral or weakly acidic conditions occurs apparently not via chelation but due to concerted action of the negatively charged carboxylate oxygen atoms of the anions, opening for increased selectivity in binding and release. Composition of the

complexes corresponds to the $\text{RE}^{3+} : \text{L} = 1:1$ ratio according to the quantification of the adsorption that quickly reaches the equilibrium. Bigger cations require much higher ligand density and thus the uptake capacity towards them in real systems is lower as not all donor atoms can become accessible for their binding, which explains the observed higher capacity and selectivity of the complexone-derived adsorbent towards smaller (heavier) REE.

The obtained new magnetic nano adsorbent hybrid material was stable for more than half-a-year under acidic conditions which is important for use of such materials in industrial purposes for desorbing the lanthanides in acidic conditions.

Experimental

Chemicals. For the synthesis of nanoparticles FeCl_3 (98%), FeCl_2 (97%), NH_4OH (25%) and TEOS (98%), ethanol (99.5%) were purchased from Sigma-Aldrich. For the synthesis of organic ligands, IDA (iminodiacetic acid) (98%), SOCl_2 (95%), iodopropyltriethoxysilane (IPTES) (98%), DIPEA (99%) were purchased from Sigma-Aldrich. Rare earths salts, $\text{La}(\text{NO}_3)_3 \cdot 6\text{H}_2\text{O}$, $\text{Dy}(\text{NO}_3)_3 \cdot 6\text{H}_2\text{O}$, $\text{Nd}(\text{NO}_3)_3 \cdot 6\text{H}_2\text{O}$ were purchased from Sigma-Aldrich. The solvents were dried applying conventional techniques before using for the reaction. All experiments were performed in Schlenk equipment using $\text{N}_2(\text{g})$ atmosphere. In order to purify the reaction mixtures, flash column chromatography was used in thick glass columns and “flash grade” silica gel (Merck 230-400 mesh, 0.040-0.063 mm). Purification of the compounds and also investigation of the reaction progress was monitored by TLC on Merck Silica gel 60 F254 as aluminium sheets.

Synthesis of Fe_3O_4 nanoparticles.

Magnetite was prepared by co-precipitation of iron(II) and iron(III) chlorides with ammonia in nitrogen atmosphere.³³ The obtained Fe_3O_4 particles were spherical with an average diameter of about 12 nm according to TEM, and specific surface area of about $96 \text{ m}^2 \text{ g}^{-1}$.

Synthesis of SiO_2 coated $\gamma\text{-Fe}_2\text{O}_3$ nanoparticles.

Fe_3O_4 nanoparticles (100 mg) were dispersed in milli-Q water (32 mL) and sonicated for 20 min. Then, dispersed solution was mixed with ethanol (160 mL) while slowly adding NH_4OH (4 mL, 25%) solution. After that, TEOS (1.6 mL) was added drop wise to achieve $\text{SiO}_2:\text{FeO}_x = 6:1$. The mixture was stirred for 20 hours.¹⁷ Magnetic nanoparticles were separated from the result mixture with magnet. It has been demonstrated earlier by XANES spectroscopy that this procedure is associated with quantitative transformation of Fe_3O_4 into $\gamma\text{-Fe}_2\text{O}_3$. Silica coated $\gamma\text{-Fe}_2\text{O}_3$ nanoparticles were washed for 3 times with dd. H_2O (25 mL) and 2 times with ethanol (25 mL) and centrifuged at 10,000 rpm for 10 min. Then, nanoparticles were dried under nitrogen atmosphere.

Synthesis of IDA conjugated $\gamma\text{-Fe}_2\text{O}_3\text{-SiO}_2$ nanoparticles.

The synthesized silica coated $\gamma\text{-Fe}_2\text{O}_3$ nanoparticles (1.2 g) were dispersed in anhydrous toluene (20 mL). The previously synthesized IDA ligand, $(\text{C}_2\text{H}_5\text{O})_3\text{Si}(\text{CH}_2)_3\text{N}(\text{CH}_2\text{COOCH}_3)_2$ obtained by condensation between iodopropyl triethoxysilane and iminodiacetic acid dimethyl ester according to³⁴ (100 mg, 0.62 mmol), was added to the first solution. The reaction mixture was refluxed overnight under nitrogen. After that, IDA bonded $\gamma\text{-Fe}_2\text{O}_3\text{-SiO}_2$ nanoparticles were washed for 3 times with toluene (25 mL) and 2 times with ethanol (25 mL) and centrifuged at 10,000 rpm for 10 min. Then, nanoparticles were dried under nitrogen atmosphere. According to the solid state

NMR investigation of the analogous silica particles free from magnetic component, the ester groups are in this case fully hydrolysed leaving only carboxylic functions.

Introduction of the lanthanide (Dy^{3+} , Nd^{3+} and La^{3+}) ions into the dispersion of organic ligand grafted SiO_2 nanoparticles (static adsorption).

As stock solutions, 0.2 M solutions (25 mL) of $\text{M}(\text{NO}_3)_3$, where $\text{M} = \text{La}$, Nd , Dy , were prepared. To 50 mg of organic ligand-grafted $\gamma\text{-Fe}_2\text{O}_3\text{-SiO}_2$ nanoparticles, 5 mL of lanthanide salt solutions (single RE or pair of RE in 1:1 ratio) were added on quick shaking and at room temperature for chosen time. The lanthanide grafted hybrid nanoparticles were centrifuged at 10,000 rpm for 10 minutes and washed 3 times with water (20 mL) and 2 times with ethanol (20 mL). The nanoparticles were dried under $\text{N}_2(\text{g})$ at room temperature.

Desorption experiments for the Dy^{3+} and Nd^{3+} ions from the nanoparticle based adsorbent.

30 mg of SiO_2 grafted with L3 bearing trivalent RE cations adsorbed according to the technique above, were mixed with 5 ml 1M HCl and 15 ml MilliQ water resulting in a mixture with final pH= 1. The mixtures were shaken for 24 h in an orbital shaker and separated by centrifugation. The collected solutions were neutralized until pH = 6 through evaporation and redilution by MilliQ water until original volume. After neutralization the RE ions were titrated with 5 mM Trilon B using xylenol orange as indicator. Quantification of RE ratios in adsorption and desorption was carried out by EDS analysis and averaged of at least 5 measurements for 5000x magnification. For details, please, see the Supplementary materials, Table TS1.

Complexometric titration of lanthanides (Dy^{3+} , Nd^{3+} , La^{3+}) in mother liquor over IDA bonded silica covered Fe_3O_4 nanoparticles.

As stock solutions, 0,0215 M $\text{Dy}(\text{NO}_3)_3$, 0,0125 M $\text{Nd}(\text{NO}_3)_3$ and 0,022 M $\text{La}(\text{NO}_3)_3$ were prepared. To 50 mg of $\text{Fe}_3\text{O}_4\text{-SiO}_2$ NPs, a calculated amount of lanthanide salt solution (corresponding to the moles of IDA grafted on the surface) was added. NaNO_3 1M was added up to a final concentration of 0.1 M in a total volume of 20 mL, which was completed with distilled water. The mixtures were then sonicated in order to disperse the nanoparticles in the solution and they stayed in static sorption conditions for different times (2, 8, 24 and 48 hours). After the corresponding time, the mixtures were poured into centrifuge tubes, centrifuged at 10,000 rpm for 10 minutes and washed once with distilled water (20 mL). Both the first and the washing solutions were collected in an Erlenmeyer and the solid sorbent was dried under N_2 (g) at room temperature. The collected solutions were titrated with Trilon B 5 mM using xylenol orange as indicator. Trilon B complexates metals in a 1:1 ratio, therefore the amount of lanthanides adsorbed to the surface of the $\text{Fe}_3\text{O}_4\text{-SiO}_2$ NPs could be calculated by subtraction, since the initial amount is known and the remaining amount in solution is determined by titration. The titrations were repeated in triplicate for control of reproducibility.

Synthesis of molecular model compounds (IDA-RE $^{3+}$). Iminodiacetic acid (IDA) (100 mg, 0.75 mmol) was dissolved in dd. H_2O (5 mL). To this solution, $\text{RE}(\text{NO}_3)_3$ (0.75 mmol) was added and stirred overnight. The result solution was left for crystallization in open air for a week. Concentration of solutions on evaporation produced syrap-like media from which clashes of needle-shaped crystals slowly formed on further drying. The produced complexes were identified as $[\text{Dy}(\text{OCOCH}_2\text{NH}_2\text{CH}_2\text{COO})(\text{H}_2\text{O})(\text{NO}_3)]^+(\text{NO}_3^-)$ (**1**) and $[\text{La}(\text{OCOCH}_2\text{NH}_2\text{CH}_2\text{COO})(\text{H}_2\text{O})_4]_2^{2+} \cdot (\text{NO}_3^-)_3 \cdot [\text{OCOCH}_2\text{NH}_2$

$\text{CH}_2\text{COO}]^- \cdot 2\text{H}_2\text{O}$ (**2**) by X-ray single crystal studies (see above).

Synthesis of molecular model compounds (IDA-RE $^{3+}$). Iminodiacetic acid (IDA) (100 mg, 0.75 mmol) was dissolved in dd. H_2O (5 mL). To this solution, $\text{RE}(\text{NO}_3)_3$ (0.75 mmol) was added and stirred overnight. The result solution was left for crystallization in open air for a week. Concentration of solutions on evaporation produced syrap-like media from which clashes of needle-shaped crystals slowly formed on further drying. The produced complexes were identified as $[\text{Dy}(\text{OCOCH}_2\text{NH}_2\text{CH}_2\text{COO})(\text{H}_2\text{O})(\text{NO}_3)]^+(\text{NO}_3^-)$ (**1**) and $[\text{La}(\text{OCOCH}_2\text{NH}_2\text{CH}_2\text{COO})(\text{H}_2\text{O})_4]_2^{2+} \cdot (\text{NO}_3^-)_3 \cdot [\text{OCOCH}_2\text{NH}_2\text{CH}_2\text{COO}]^- \cdot 2\text{H}_2\text{O}$ (**2**) by X-ray single crystal studies (see above).

Characterization.

$^1\text{H-NMR}$ and $^{13}\text{C-NMR}$ spectra were recorded on Bruker Avance spectrometer operating at 600 MHz for $^1\text{H-NMR}$ and 150 MHz for $^{13}\text{C-NMR}$ in CDCl_3 solvent with tetramethylsilane (TMS) as internal. All spectra were recorded at 25° C and coupling constants (J values) are given in Hz. Chemical shifts are given in parts per million (ppm). The ^{29}Si magic-angle spinning (MAS) cross polarization (CP) NMR and ^{13}C CP/MAS NMR spectra were recorded on a Bruker Avance III 400 (9.4 T) spectrometer at 79.49 and 100.62 MHz, respectively. ^{29}Si MAS NMR spectra were recorded with 2 ms (tip angle ca. 30°) rf pulses, a recycle delay of 60 s and 5.0 kHz spinning rate. ^{13}C CP/MAS NMR spectra were recorded with 4 ms ^1H 90° pulses, 2 ms contact time, a recycle delay of 4 s and at a spinning rate of 8 kHz. Chemical shifts are quoted in ppm from tetramethylsilane (TMS). SEM-EDS studies were performed with Hitachi TM-1000- μ -DeX tabletop scanning electron microscope. TEM analyses were performed with a JEOL brand JEM 2100F model transmission electron microscope operating at 200 kV. The samples (about 1 mg/mL) were prepared in ethanol solution and dropped onto a carbon-coated copper grid and dried at room temperature. Fourier-transform infrared (FTIR) spectra of the produced nanoparticles were recorded as KBr pellets on the Perkin-Elmer Spectrum 100 instrument. Thermogravimetric analyses (TGA) were carried out using Perkin-Elmer Pyris 1 instrument under air atmosphere at a heating rate of 5°C/min in the temperature interval 25-600°C.

Crystallography.

Data collection for single crystals of **1** and **2** was carried out at room temperature using MoK_α radiation ($\lambda = 0.71073 \text{ \AA}$) with Bruker SMART Apex-II CCD diffractometer. The details of data collection and refinement are summarized in Table 3.

The structures were solved by direct methods. The positions of metal atoms were identified from the initial solution and all other non-hydrogen atoms were located in difference Fourier syntheses. All non-hydrogen atoms were refined first in isotropic and then in anisotropic approximation. Positions of the hydrogen atoms were calculated geometrically for the NH_2^+ -groups and CH_2 -fragments while the hydrogen atoms at the oxygen atoms were found in difference Fourier syntheses. Practically all H atoms were successfully located and included into the final refinement in isotropic approximation. The refinement converged at low R-values (see Table 3), proving that structure of both the cationic coordination polymers and the anionic fragments and neutral molecules in the interlayer spaces have been located and refined in a correct way. Because of the considerable disorder the treatment of the data required manual introduction of partial occupancies for the structure of **2**, resulting in reporting a large number of restraints. Some

residual electron density in the proximity of metal atom in the structure of **1** might have resulted from most probably not fully successful adsorption correction.

Table 3 Crystal data and diffraction experiments' details for compounds **1** and **2**.

Chemical composition	C ₄ H ₁₀ N ₃ O ₁₂ Dy(1)	C ₁₂ H ₂₅ N ₆ O ₃₁ La ₂ (2)
Formula weight	454.65	1014.10
Crystal system	Triclinic	Orthorhombic
Space group	P-1	Cmcm
μ/mm^{-1}	6.337	2.696
R1	0.0456	0.0321
wR2	0.1219	0.0679
a/Å	7.9728(17)	18.835(8)
b/Å	8.7556(19)	9.133(4)
c/Å	9.748(2)	19.034(8)
$\alpha/^\circ$	66.953(2)	90
$\beta/^\circ$	88.290(2)	90
$\gamma/^\circ$	73.131(2)	90
V/Å ³	596.5(2)	3274(2)
T/K	296(2)	296(2)
Z	2	4
Number of independent reflections	2266 [R(int) = 0.0323]	1675 [R(int) = 0.0305]
Number of observed reflections	2225 [I > 2 σ (I)]	1107 [I > 2 σ (I)]

X-ray powder (XRD) experiments were carried out with the same instrument. The data collection and reduction were made using Bruker Apex-II program package and the evaluation and identification of phases was carried out with Bruker EVA-12 program.³⁵

Acknowledgements

The research leading to these results has received funding from the European Community's Seventh Framework Programme ([FP7/2007-2013]) under grant agreement n°309373. This publication reflects only the author's view, exempting the Community from any liability". Project web site: www.eurare.eu. The authors are also indebted to the Swedish Research Council (Vetenskapsrådet) for the support of the project "Molecular precursors and molecular models of nanoporous materials".

Notes and references

^a Department of Chemistry and Biotechnology, BioCenter, Swedish University of Agricultural Sciences, Box 7015, 75007 Uppsala, Sweden, E-mail: gulaim.seisenbaeva@slu.se

Electronic Supplementary Information (ESI) available: the data of XRD, TGA and EDS characterization of ligand grafted nanoparticles. See DOI: 10.1039/b000000x/

Supplementary crystallographic data are available from the CCDC, 12 Union Road, Cambridge CB2 1EZ, UK on request, quoting the deposition numbers CCDC 1018502 and 1018503 for **1** and **2** respectively.

- P. Zhang, L. Zhang, C. Wang, S. Xue, S-Y. Lin, J. Tang, *J. Am. Chem. Soc.*, 2014, **136**, 4484-4487.
- D. Parker, Y. Bretonniere, *Mol. Imagin*, 2005, **49**, 123-146.
- T. Jin, S.Inoue, K. Machida, G. Adachi, *J. Electrochem. Soc.*, 1997, **144**(11), 4054-4058.
- M. Shibusaki, N. Yoshikawa, *Chem. Rev.*, 2002, **102**, 2187-2209.
- J.C.G. Bunzli, C. Piguet, *Chem. Rev.*, 2002, **102**, 1897-1928.
- W. Yantasee, G.E. Fryxell, R.S. Addleman, R.J. Wiacek, V. Koonsiripaiboon, J. Xu, K.N. Raymond, *J. Hazard. Mater.*, 2009, **168**, 1233-1238.
- (a) R.S. Addleman, M. Douglas, R.D. Rutledge, W. Chouyyok, J.D. Davidson, G.E. Fryxell, J.M. Schwantes, *Environ. Sci. Technol.*, 2012, **46**, 11251-11258; (b) D. Dupont, W. Brulot, M. Bloemen, T. Verbiest, K. Binnemans, *Appl. Mat. & Inter.*, 2014, **6**, 4980-4988.
- E.H. Smith, *Water Research*, 1996, **30**, 2424-2434.
- (a) S.J. Soenan, M.D. Cuyper, S.C. Smedt, K. Braeckmans, *Methods in enzymology*, 2012, **509**, 195-224; (b) K. Wilkinson, B. Ekstrand-Hammarström, L. Ahlinder, L.; K. Guldevall, R. Pazik, L. Kepinski, K.O. Kvashnina, S.M. Butorin, H. Brismar, B. Onfelt, L. Osterlund, G.A. Seisenbaeva, V.G. Kessler, *Nanoscale*, 2012, **4**(78), 7383-7393.
- C.Z. Huang, B. Hu, *Spectrochim Acta B Atomic Spectrosc.*, 2008, **63**, 437-444.
- P.I. Girginova, A. Daniel de Silva, C.B. Lopes, P. Figueira, M. Otero, V.S. Amaral, E. Pereira, T. Trindade, *J. Colloid Interface. Sci.*, 2010, **345**, 234-240.
- S. Shin, J. Jang, *Chem. Comm.*, 2007, 4230-4232.
- P. Xu, M.G. Zeng, D.L. Huang, C.L. Feng, S. Hu, M.H. Zhao, C. Lai, Z. Wei, C. Huang, G.X. Xie, Z.F. Liu, *Sci. Total Envir.*, 2012, **424**, 1-10.
- A-H. Lu, E.L. Salabas, F. Schüth, *Angew Chem. Int. Ed.*, 2007, **46**, 1222-1244.
- R. Pogorilyi, I.V. Melnyk, Y.L. Zub, S. Carlson, G. Daniel, P. Svedlindh, G.A. Seisenbaeva, V.G. Kessler, *RSC Adv.*, 2014, **4**, 22606-22612.
- (a) M. Stjernerdaahl, M. Andersson, H.E. Hall, D.M. Pajeroski, M.W. Meisel, R.S. Duran, *Langmuir*, 2008, **24**, 3532-3536; (b) S.H. Im, T. Herricks, Y.T. Lee, Y. Xia, *Chem. Phys. Lett.*, 2005, **401**, 19-23.
- W. Stöber, A. Fink, E. Bohn, *J. Colloid Interface Sci.*, 1968, **26**, 62.
- M. Abbas, B.P. Rao, M.N. Islam, S.M. Naga, M. Takahashi, C. Kim, *Ceramics Int.*, 2014, **40**, 1379-1385.
- (a) A.B. Chin, I.I. Yaacob, *J. Mater. Process. Technol.*, 2007, 191, (b) S. Santra, R. Tapeç, N. Theodoropoulou, J. Dobson, A. Hebard, W.H. Tan, *Langmuir*, 2001, **17**, 2900-2906; (c) E. Effati, B. Pourabbas, *Powder Technology*, 2012, **219**, 276-283.
- (a) C. Albornoz, S.E. Jacobo, *J. Magn. Magn. Mater.*, 2006, **305**, 12-15; (b) E.H. Kim, H.S. Lee, B.K. Kwak, B.K. Kim, *J. Magn. Magn. Mater.*, 2005, **289**, 328-330.
- J. Wan, X. Chen, Z. Wang, X. Yang, Y. Qian, *J. Cryst. Growth.*, 2005, **276**, 571-576.
- M. Kimata, D. Nakagawa, M. Hasegawa, *Powder Technol.*, 2003, **132**, 112-118.

- 23 G. Salazar Alvarez, M. Muhammed, A.A. Zagorodni, *Chem. Eng. Sci.*, 2006, **61**, 4625-4633.
- 24 S. Basak, D.-R. Chen, P. Biswas, *Chem. Eng. Sci.*, 2007, **62**, 1263-1268.
- 25 I. Martinez-Mera, M.E. Espinosa-Pesqueira, R. Perez-Hernandez, J. Arenas-Alatorre, *Mater. Lett.*, 2007, **61**, 4447-4451.
- 26 S.-J. Lee, J.-R. Jeong, S.-C. Shin, J.-C. Kim, J.-D. Kim, *J. Magn. Mater.*, 2004, **282**, 147-150.
- 27 F. Gonzaga, G. Yu, M.A. Brook, *Chem. Comm.*, 2009, 1730-1732.
- 28 V. Vinciguerra, R. Bucci, F. Marini, A. Napoli, *J. Thermal Anal. Calorimetry*, 2006, **83**, 475-478
- 29 (a) C. Kremer, P. Morales, J. Torres, J. Castiglioni, J. González-Platas, M. Hummert, H. Schumann, S. Domínguez, *Inorg. Chem. Comm.*, 2008, **11**, 862-864; (b) L.M. Zhang, N.Q. Yu, K.H. Zhang, R.S. Qiu, Y.X. Zhao, W.C. Rong, H. Deng, *Inorg Chim Acta*, 2013, **400**, 67-73.
- 30 (a) J. Albertsson, Å. Oskarsson, *Acta Chem Scand.*, 1968, **22**, 1700-1702; (b) Å. Oskarsson, *Acta Chem. Scand.*, 1971, **25**, 1206-1216; (c) Å. Oskarsson, *Acta Chem. Scand.*, 1972, **26**, 2126-2128.
- 31 (a) P. Werndrup, V.G. Kessler, *Inorg. Chem. Comm.*, 2004, **7**, 588-591; (b) O. Viotti, A. Fischer, G.A. Seisenbaeva, V.G. Kessler, *Inorg. Chem. Comm.*, 2010, **13**, 774-777; (c) O. Viotti, G.A. Seisenbaeva, V.G. Kessler, *Inorg. Chem.*, 2009, **48**, 9063-9065.
- 32 (a) J. Wang, G.G. Gao, Z.H. Zhang, X.D. Zhang, Y.J. Wang, *J. Coord. Chem.*, 2007, **60**(20), 2221-2241; (b) X.M. Zhuang, Q.P. Long, J. Wang, *Acta Cryst. E*, 2010, **E66**, m1436; (c) J.Q. Gao, T. Wu, J. Wang, Y. Baia, S.J. Wang, Y. N. Xu, Y. Li, X.D. Zhang, *Russ. J. Coord. Chem.*, 2012, **38**(7), 491-500; (d) J. Wang, Y. Wang, X.D. Zhang, Z.H. Zhang, Y. Zhang, L.P. Kang, H. Li, *J. Coord. Chem.*, 2005, **58**(11), 921-930.
- 33 Z. Ma, Y. Guan, H. Liu, *J. Magn. Mater.*, 2006, **301**, 469-477.
- 34 J.I. Zink, D. Tarn, *Inorg. Chem.*, 2013, **52**, 2044-2049.
- 35 Bruker, APEX2 (Version 2008.1-0) and EVA (Version 12). Bruker AXS Inc., Madison, Wisconsin, USA, 2008.